Controlling distant contacts to reduce disease spreading on disordered complex networks

Ignacio A. Perez[*]

Instituto de Investigaciones Físicas de Mar del Plata (IFIMAR)-Departamento de Física,

FCEyN, Universidad Nacional de Mar del Plata-CONICET,

Funes 3350, (7600) Mar del Plata, Argentina.

Paul A. Trunfio

Physics Department and Center for Polymer Studies,

Boston University, Boston, Massachusetts 02215, USA

Cristian E. La Rocca and Lidia A. Braunstein

Instituto de Investigaciones Físicas de Mar del Plata (IFIMAR)-Departamento de Física,

FCEyN, Universidad Nacional de Mar del Plata-CONICET,

Funes 3350, (7600) Mar del Plata, Argentina. and

Physics Department and Center for Polymer Studies,

Boston University, Boston, Massachusetts 02215, USA

Abstract

In real social networks, person-to-person interactions are known to be heterogeneous, which can affect the way a disease spreads through a population, reaches a tipping point in the fraction of infected individuals, and becomes an epidemic. This property, called *disorder*, is usually associated with contact times between individuals and can be modeled by a weighted network, where the weights are related to normalized contact times ω. In this paper, we study the SIR model for disease spreading when both close and distant types of interactions are present. We develop a mitigation strategy that reduces only the time duration of distant contacts, which are easier to alter in practice. Using branching theory, supported by simulations, we found that the effectiveness of the strategy increases when the density f_1 of close contacts decreases. Moreover, we found a threshold $\tilde{f}_1 = T_c/\beta$ below which the strategy can bring the system from an epidemic to a non-epidemic phase, even when close contacts have the longest time durations.

Keywords: Complex network, Epidemic modeling, Percolation, SIR model

* ignacioperez@mdp.edu.ar

I. INTRODUCTION

In recent centuries, changes in social contact patterns have caused infectious diseases to propagate more rapidly and become more widespread [1]. The population growth in urban zones and the increasing speed and efficiency of air travel have allowed diseases to spread over long distances within months or even weeks. Examples include the 1918 Spanish flu [2], the 2009 A(H1N1) influenza epidemic [3], the 2014 Ebola epidemic [4], and the recent measles outbreak in Israel that propagated to New York [5]. Prior research has indicated that due to the increased resistance of bacteria to drugs [6], climate change [7, 8] and the deforestation of sylvan areas [9], the number of diseases will continue to increase. In this context, mathematical models allow epidemiologists and sanitary authorities to understand propagation processes, predict their effect on healthy populations, and evaluate the effectiveness of different mitigation strategies. Although many models consider full mixing, in which all individuals in a population interact with each other [1], this assumption does not reflect a realistic situation where an individual has a limited number of interactions and where it can vary between individuals. For that reason, in recent decades, researchers have begun to model epidemic processes using complex networks, in which a node (an individual) has a probability $P(k)$ of being connected with k different nodes (neighbors) with $k_{\min} \leq k \leq k_{\max}$, where $k_{\min}$ and $k_{\max}$ are the minimum and maximum connectivity, respectively; they have found that connection patterns strongly affect the spreading of a disease [10–15].

The Susceptible-Infected-Recovered (SIR) model [1, 10, 11, 16] is a simple representation of non-recurrent diseases, where individuals acquire permanent immunity once they stop being ill. Examples include influenza A(N1H1), measles and pertussis. In this model, an individual is either *susceptible* (able to be infected), *infected* (can propagate the disease), or *recovered* (has either acquired an immunity or has died, thereby no longer propagating the disease). In the discrete-time Reed-Frost model [17], at each time step, infected individuals spread the disease to susceptible neighbors, with probability β, and recover t_r time steps after being infected. The effective probability of infection is, thus, given by the transmissibility $T = 1 - (1 - \beta)^{t_r}$. The process ends when there are no more infected individuals; the system has reached the steady state. The SIR model, at the steady state, exhibits a second-order phase transition where the fraction R of recovered individuals is the order parameter, while T is the control parameter. Below a critical threshold $T = T_c$, the disease reaches

3

only a small fraction of the population, but when $T > T_c$ it becomes an epidemic [10, 18–20]. Studies have shown that the steady state of the SIR model is related to link percolation [10, 16, 19, 21]. In the SIR model, links are occupied with probability p since the propagation of the disease from an infected to a susceptible individual, is equivalent to occupying that link via link percolation (i.e., $T \equiv p$). Above a critical threshold $p = p_c$, a giant component (GC) of the same order of magnitude than the system size N emerges, whereas below p_c there are only finite clusters. The fraction P_∞ of nodes belonging to the GC is the order parameter of a second-order phase transition, with R from the SIR model mapping into P_∞ [10]. Because the SIR process only produces one cluster of nodes (those reached by the disease), realizations with $R < s_c$ are neglected for the mapping to exist [20]. For complex networks $p_c = 1/(\kappa - 1) = T_c$, where $\kappa = \langle k^2 \rangle / \langle k \rangle$; $\langle k \rangle$ and $\langle k^2 \rangle$ are the first and second moments of the distribution $P(k)$, respectively [10, 16].

There are different strategies proposed to contain the spreading of diseases. Vaccination is one of the more studied and it is highly efficient in providing immunity [22–24], although vaccines are often expensive and not always available. In this context, non-pharmacological strategies are needed to protect populations. For instance, quarantine is one of the most effective, however complete isolation has a deleterious effect on the economy of a region, and it is difficult to implement in a large population. Thus, "social distancing" [25–29], i.e., reducing the contact times of interactions between individuals, is often implemented and carried out, for instance, by partial closure of schools and offices, and restriction of travel [30].

In this paper, we focus on social distancing interventions to develop a mitigation strategy that can help in reducing the number of infected people. One way for studying these kinds of strategies is to examine the heterogeneity in the contact times between individuals. Most research that studies the SIR model assumes that the infection probability is unique, which means that all individuals interact with their neighbors in the same way. This has been disproven by several experiments on real social networks [31–33]. For example, "face-to-face" experiments [31, 33] have shown that, in some cases, the time duration of the contacts between individuals follow a power-law distribution. This heterogeneity is called "disorder", and it can be modeled using weighted networks, in which weights depend on the normalized contact times ω of the interactions. Previous research [27, 34] obtains ω values from a theoretical power law distribution with broadness a (the larger the parameter a, the shorter

the contact times), mimicking the results of "face-to-face" experiments [31, 33]. Among other outcomes, they found a delay in spreading of diseases as the broadness a increases [27], thereby permitting sanitary authorities to implement earlier interventions [34].

Unlike proposals of previous models, differing classes of human interactions arise in real social networks. From the most prolonged relationships (e.g., friendships, family, and coworkers), to the briefest interactions (e.g., neighbors in transport and commerce), contacts between individuals require a better distinction when modeling a social network. Motivated by this real-world reality, we study the propagation of diseases among a population with two coexisting types of interactions, which we distinguish by their mean contact time. More precisely, interactions can be close or distant with a larger or shorter mean contact time, respectively. Each type of interaction has a distribution of contact times governed by its own broadness a, which defines the mean contact time. We use branching theory, supported by extensive simulations, to explore a social distancing strategy that consists of reducing only the mean contact time of distant interactions. We propose this strategy because, generally, people are less prone to trim their more intimate or necessary contacts, while distant contacts are more easily controlled.

II.   MODEL AND SIMULATIONS

We construct complex networks of N nodes as a substrate for the propagation of a disease, by using the Molloy-Reed algorithm [35]. We build two types of networks with different degree distributions. First, $P(k) = e^{-\langle k \rangle} \langle k \rangle^k / k!$—an Erdös-Rényi network (ER)—in which $\langle k \rangle$ is the average number of neighbors of each node, and second, $P(k) = Ck^{-\lambda} e^{-k/k_c}$— a scale-free network (SF)—with exponential cutoff k_c and normalization constant C. ER networks are homogeneous because their nodes have a number of neighbors mostly around the mean value of the distribution, whereas SF networks are heterogeneous and hence nodes have a greater amplitude in their connectivities, with many nodes of low connectivity and only a few nodes of high connectivity (hubs).

We use the SIR model described in Sec. I to simulate the spreading of the disease, but we assume that the infection probability is related to the contact times between individuals, i.e., the more time a susceptible individual spends with an infected person, the higher the probability they will also become infected. Thus, the infection probability is $\beta\omega$, where
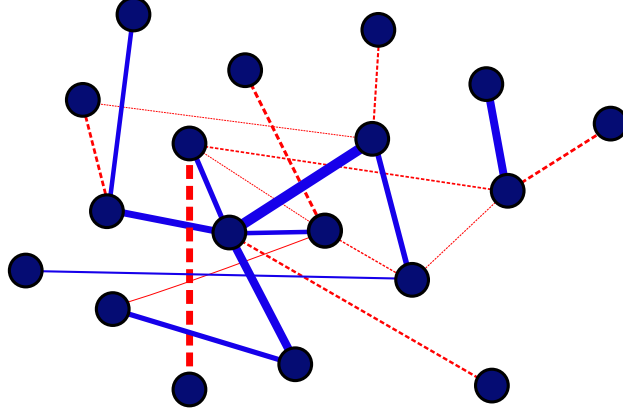
5

FIG. 1: Schematic of the network constructed. The different thicknesses of the segments represent the heterogeneity of the normalized contact times ω between individuals. Contact times belonging to the density f_1 (—), with $a_1 < a_2$, are usually longer than those belonging to the complementary density $f_2 = 1 - f_1$ (- - -).

a fixed β represents the intrinsic virulence of the disease and ω represents the normalized contact time between individuals. We also assume that the contact times are heterogeneous, and hence we use a weighted network, in which we characterize links (contacts) by weights $\beta\omega$. As in "face-to-face" experiments [31], in which contact times follow a power law distribution, we take ω from a theoretical distribution of contact times $P(\omega) = 1/a\omega$, where $\omega \,\epsilon\, [e^{-a}, 1]$ [27, 34]. The parameter a is called *disorder intensity*, as it controls the width of the distribution. For fixed a, we set $\omega = e^{-ar}$, where r is randomly selected from a uniform distribution over the interval $[0, 1]$ [36]. We also separate the contacts into two complementary parts, (i) a fraction or density f_1 of links with a distribution of contact times with disorder intensity a_1 and (ii) a density $f_2 = 1 - f_1$ with a distribution with disorder intensity a_2, for $0 < f_1 < 1$. In Fig. 1 we show the density f_1 of interactions corresponding to the distribution with disorder intensity a_1, $a_1 < a_2$ (blue continuous lines). On average, the interactions corresponding to the density f_1 have longer contact times than the ones corresponding to the density $f_2 = 1 - f_1$ (red dashed lines), indicated by the thickness of the segments. Our approach allows for modeling realistic populations in which different kinds of interactions can emerge. For instance, when $a_1 < a_2$ we can distinguish between close and distant contacts, where a_1 and a_2 are the disorder intensities of close contacts (longer average contact times) and distant contacts (shorter average contact times), respectively. As distant contacts are easier to control in practice, we propose a mitigation strategy that

focuses on modifying them to reduce the scope of the disease. In Sec. III we apply ourselves to this task.

When the propagation starts at $t = 0$, all individuals are susceptible except for one randomly-infected *patient zero*. With probability $\beta\omega$, at each time step, infected individuals propagate the disease to their susceptible neighbors, where ω is initially fixed and depends on the interaction between individuals. Each infected individual recovers after a time t_r since it was infected. The spreading process ends when there are no more infected individuals, and all are either susceptible or recovered. At this steady state the fraction R of recovered individuals for a given value of the transmissibility T indicates the extent of the disease, since all recovered individuals were previously infected. Recall that only realizations with $R > s_c$ are taken into account, where s_c is the threshold that distinguish an epidemic $(R > s_c)$ from an outbreak $(R < s_c)$.

Introducing disorder in the contact times changes the transmissibility formula [34]. In our model we must account for the densities f_1 or $1 - f_1$ of links that have weights ω corresponding to the distribution with a disorder intensity of a_1 or a_2, respectively. Then the transmissibility $T_{a_1 a_2}$ for a given virulence β and recovery time t_r is

$$T = T_{a_1 a_2} = f_1 T_{a_1} + (1 - f_1) T_{a_2}, \tag{1}$$

where

$$T_{a_i} = \sum_{t=1}^{t_r} \frac{(1 - \beta e^{-a_i})^t - (1 - \beta)^t}{a_i t} \tag{2}$$

is the transmissibility of a disease in a network with a unique distribution of contact times $(f_1 = 0$ or $f_1 = 1)$, with disorder intensity a_i, $i = 1, 2$ [34]. Note that the transmissibility $T_{a_1 a_2}$ is a decreasing function of the intensities a_1 and a_2, because for higher values of a_1 or a_2 the range of values for ω allowed in each distribution of disorder expands, and shorter contact times become more probable. Thus, the disease is less likely to propagate. On the other hand, in the limit $a_1 \to 0$ and $a_2 \to 0$ there is no disorder, and we recover the original (homogeneous) SIR model as $T_{a_1 a_2} \to T = 1 - (1 - \beta)^{t_r}$.

When carrying out the simulations we select, for the non-disorder case, an infection probability β from the epidemic phase, i.e., $\beta > \beta_c$ or $T > T_c$. Then, we determine whether there are any pair of disorder intensities (a_1, a_2) for which there is no epidemic. In Fig. 2 we show the fraction R of recovered individuals as a function of the disorder a_2, for an ER network with $\langle k \rangle = 4$ and different values of β, where we fix $t_r = 1$, $f_1 = 0.2$ and $a_1 = 1$.
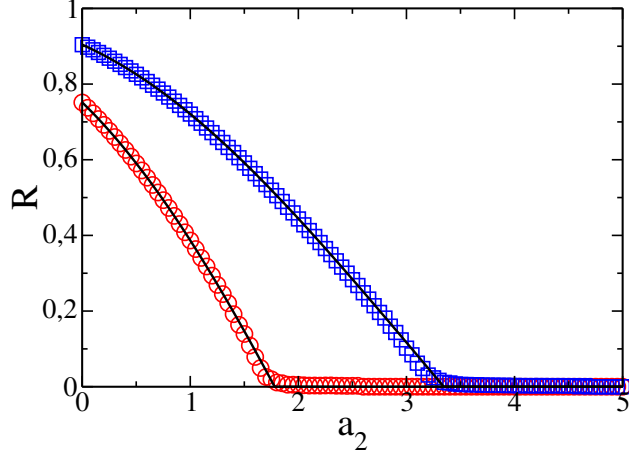
FIG. 2: Fraction R of recovered individuals at the stationary state, as a function of the disorder intensity a_2, for $\beta = 0.5$ ($\circ$) and $\beta = 0.7$ ($\square$). Note that for each value of β there is a critical value a_{2c}, such that the system is in a non-epidemic phase for $a_2 > a_{2c}$. The results of the simulations correspond to an ER network with $k_{\min} = 0$, $k_{\max} = 40$ and $\langle k \rangle = 4$, where $f_1 = 0.2$ and $a_1 = 1$. The network size is $N = 10^5$ and 10^5 realizations of the simulation are performed, with $s_c = 200$. The black curves (—) correspond to the theoretical results.

We can see that for both values of β, there is a critical value a_{2c} above which the system is in a non-epidemic phase. Note that even though we have chosen a value of β for the epidemic regime without disorder in the network, the increasing of disorder intensity a_2 reduces the spreading of the disease in the population and we obtain a non-epidemic regime. This means that epidemics could be reduced in size and even avoided if average contact times are controlled. In Sec. III we describe how to obtain the critical value for the disorder intensity a_2 and the conditions for its existence.

III. THEORY

Using the branching process formalism [10, 15, 36–38] we define the generating function of the distribution $P(k)$, $G_0(x) = \sum_k P(k)x^k$, and the generating function of the excess degree distribution $G_1(x) = \sum_k [kP(k)/\langle k \rangle]x^{k-1}$. In Fig. 2 we show the theoretical results for the fraction R of recovered individuals (black curves), obtained by solving the link percolation equations $f_\infty = 1 - G_1(1 - pf_\infty)$ and $P_\infty(p) = 1 - G_0(1 - pf_\infty)$, where f_∞ is the probability

that a branch of links expands infinitely, P_∞ is the fraction of nodes in the GC, and p is the fraction of links occupied on the network. As we stated before, the SIR model can be mapped into link percolation [10, 15, 36–38], thus, R and P_∞ are equivalent. In Fig. 2 we see that the simulation results from the SIR model with disorder present an excellent agreement with the percolation theory. The previous equations and the mapping between R and P_∞ apply in the thermodynamic limit $N \to \infty$, and for locally tree-like networks.

As stated in Sec. II, our goal is to study a mitigation strategy for a population with both close and distant interactions, in which we curtail the spreading of diseases by controlling the distant contacts. If a_1 is the disorder intensity corresponding to the distribution of close contacts and a_2 corresponds to distant contacts, then $a_1 < a_2$. Next, we use the theoretical result from the mapping that sets an equivalence between $T_{a_1 a_2}$ and p to analyze the phase space of the system, which allows us to examine our proposed mitigation strategy. In Eq. (1) we can use the critical transmissibility $T_{a_1 a_{2c}} \equiv p_c = 1/(\kappa - 1)$ to find, for $t_r = 1$,

$$\frac{1}{\kappa - 1} = f_1 \beta \frac{1 - e^{-a_1}}{a_1} + (1 - f_1)\beta\frac{1 - e^{-a_{2c}}}{a_{2c}}, \tag{3}$$

from which we can compute the critical intensity a_{2c} for different values of a_1. In Fig. 3 we show the phase diagram on the plane (a_1, a_2) for different values of f_1 and β. Because we study close and distant contacts, our interest is focused in the region of the phase space above the dashed-dotted line, which corresponds to networks such that $a_1 < a_2$. Each curve in Fig. 3 indicates the critical value a_{2c} as a function of a_1 for a given density f_1. The curves separate the epidemic phase (below) from the epidemic-free phase (on and above). We also can see that in (a) there is a point $a_2^* = a_1^* = a_c$ at which all the curves cross each other for different f_1 values, where a_c is the critical intensity for a network with a unique disorder distribution. Starting from the $a_2^* = a_1^* = a_c$ point and moving away, the critical intensity a_{2c} increases as a_1 decreases. This indicates that the longer the close contact times, the shorter the distant contact times needed to avoid the epidemic phase. In Fig. 3(b) we show that a_1 can even go to zero, which means that the close contact times can be as long as possible. In this limit we see that a_{2c} converges to a finite value $\tilde{a}_2$. Using Eq. (3) we obtain an expression for $\tilde{a}_2$,

$$T_c = f_1\beta + (1 - f_1)\beta\frac{1 - e^{-\tilde{a}_2}}{\tilde{a}_2}. \tag{4}$$

Using Eq. (4) we find that $\tilde{a}_2$ exists if $f_1 < T_c/\beta \equiv \tilde{f}_1$, otherwise the close contacts cause the system to be in an epidemic phase for any value of a_2, which means that $\tilde{a}_2$ does not exist. In
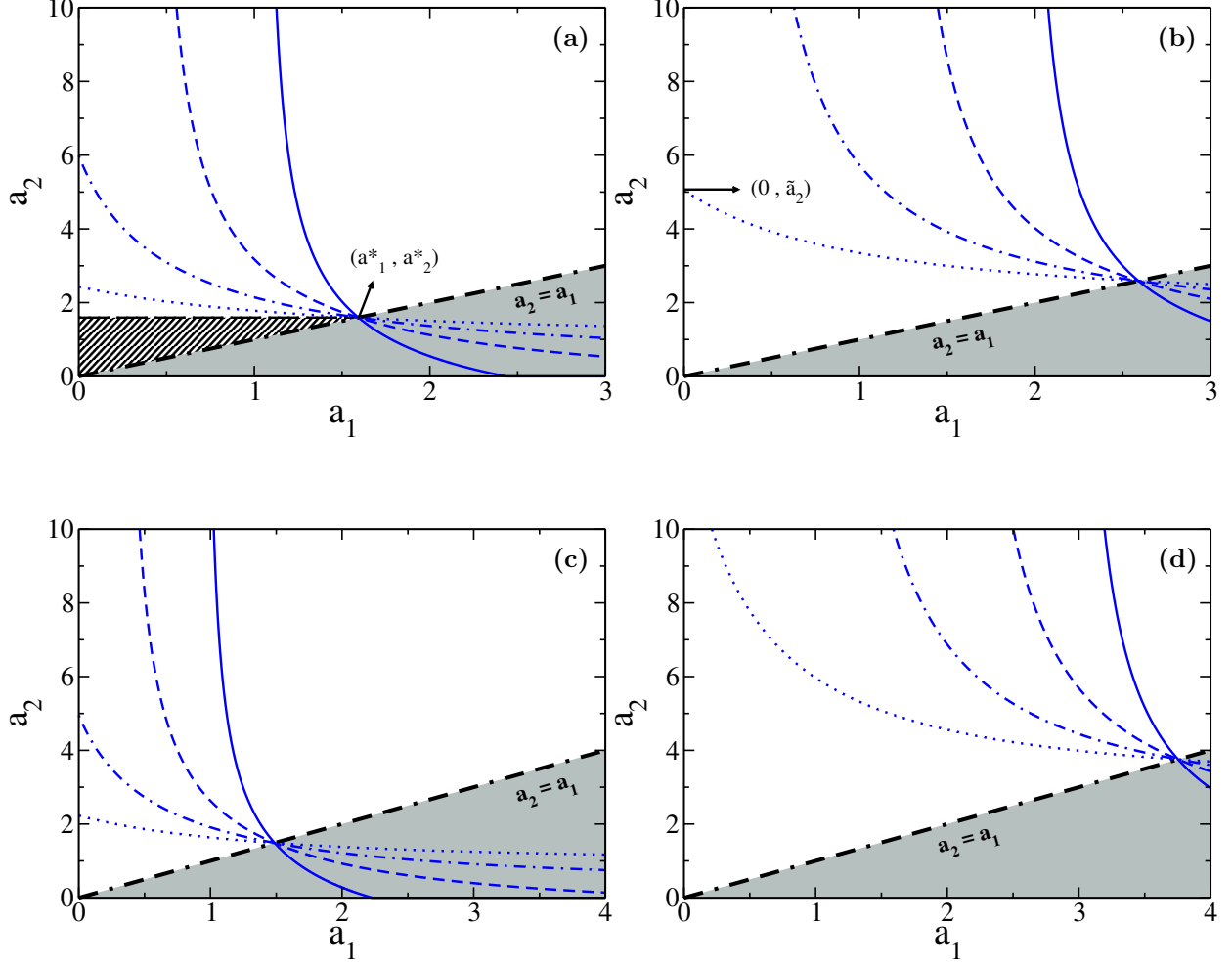
FIG. 3: Phase space of the system projected on the (a_1, a_2) plane for $t_r = 1$. Each curve represents the critical intensity a_{2c} as a function of a_1, for different densities of close contacts: $f_1 = 0.2$ (·····), $f_1 = 0.4$ (–·–·), $f_1 = 0.6$ (– – –) and $f_1 = 0.8$ (——). Below each curve, the system is in an epidemic phase, while on and above is in an epidemic-free phase. Gray regions represents networks where $a_1 > a_2$, which we are not interested in. The upper figures correspond to an ER network with $k_{\min} = 0$, $k_{\max} = 40$ and $\langle k \rangle = 4$, where (a) $\beta = 0.5$ and (b) $\beta = 0.7$. The lower figures represent a SF network with $k_{\min} = 2$, $k_{\max} = 250$, $\lambda = 2.5$ and exponential cutoff $k_c = 50$, where (c) $\beta = 0.25$ and (d) $\beta = 0.5$. The critical values of β for a non-disordered network are $\beta_c = 0.25$ and $\beta_c \approx 0.13$, for degree distributions ER and SF with exponential cutoff respectively.

10

this case, when $f_1 > \tilde{f}_1$, $a_{2c} \to \infty$ as $a_1 \to a_{1m}$ [see Eq. (3)]. Thus, distant contact times are equal to zero, and because the disease cannot pass through these contacts its corresponding transmissibility is also zero. The resulting expression for $a_1 = a_{1m}$ is then

$$T_c = f_1 \beta \frac{1 - e^{-a_{1m}}}{a_{1m}}. \tag{5}$$

Since there is no critical value a_{2c} for $a_1 < a_{1m}$, the disease is always in an epidemic phase.

Note that there is a region of the phase space (striped region) in which the disease is in an epidemic phase for all f_1 values [see Fig. 3(a)]. This region corresponds to the epidemic phase for $f_1 = 0$, i.e., when there is only one type of contacts in the network. Then, it is characterized by $T_{a2} > T_c = 1/(\kappa - 1)$.

We use these results to construct a distancing strategy for reducing the impact of a disease in a population with close and distant contacts, by controlling the duration of distant contact times. Suppose that the distribution of contact times has original disorder intensities a_1 and a_2 such that the system is in an epidemic phase. Then, if we assume that close contacts are a minor portion of the total ($f_1 < \tilde{f}_1 = T_c/\beta$), we can increase the intensity a_2 to a critical point, hence reaching a non-epidemic phase independent of the original intensities [see Fig. 4(a)]. When $f_1 > \tilde{f}_1$, the original value of the disorder intensity of close contacts determines whether we can reach the non-epidemic phase [see Fig. 4(b)]. In this case, when $a_1 < a_{1m}$ the non-epidemic phase cannot be reached by simply increasing a_2.

We also observe that, with fixed β, the critical values obtained for ER networks are lower than the ones obtained for SF networks with an exponential cutoff. We can see this result by comparing Figs. 3 (a) and (d). In homogeneous (ER) networks individuals have, on average, the same number of neighbors. Thus, there is a limit on the speed at which the disease can propagate. In contrast, the presence of hubs in heterogeneous (SF) networks causes a rapid propagation of the disease once they become infected. Therefore, these networks require higher disorder intensities (or shorter contact times) to reach a non-epidemic phase than those required in ER networks. Note also that the intrinsic virulence of the disease β modifies these critical values.

In Figs. 3(a) and 3(b), and in Figs. 3(c) and 3(d), we show that when β increases the disease becomes more aggressive, spreads more rapidly, critical intensities increase, and the epidemic phase of the disease widens.

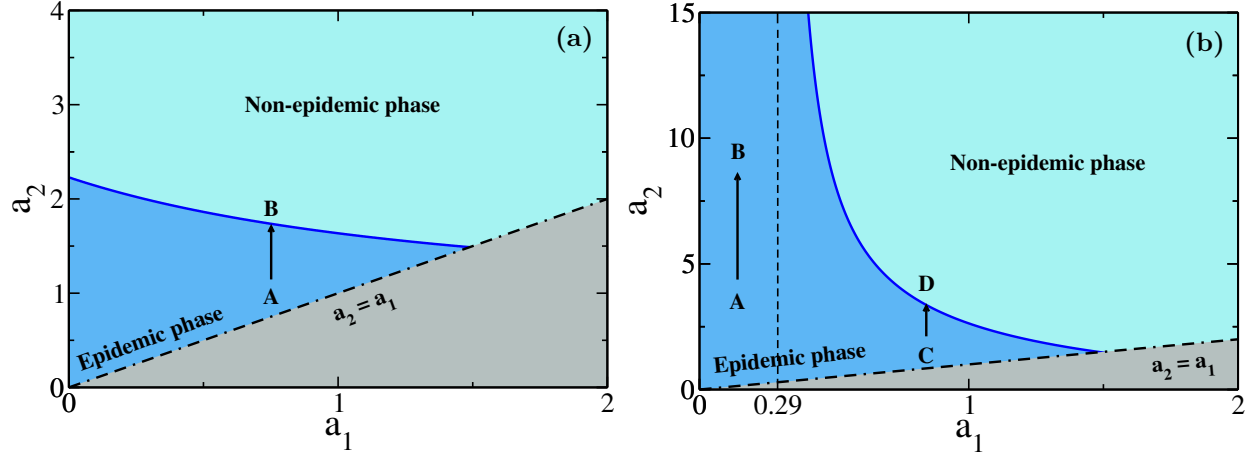Finally, we generalize the analysis for larger recovery times ($t_r > 1$). In Fig. 5 we show

FIG. 4: Schematic of the proposed strategy to halt the spreading of a disease with virulence $\beta = 0.25$. In (a) we show the case $f_1 < \tilde{f}_1 = T_c/\beta$ ($f_1 = 0.2$), where $\tilde{a}_2$ exists for $a_1 = 0$. Then, starting from any point A in the epidemic phase, by increasing a_2 we can reach the critical point in B. The opposite case ($f_1 > \tilde{f}_1$) is represented in (b) ($f_1 = 0.6$), which shows the same behavior than in (a) from point C to the critical point in D, for the case in which a_1 is originally greater than or equal to the minimum value a_{1m}, corresponding to $a_{2c} \to \infty$. Here $a_{1m} = 0.29$. The results correspond to a SF network with $k_{\min} = 2$, $k_{\max} = 250$, $\lambda = 2.5$ and exponential cutoff $k_c = 50$.

the phase space obtained from Eqs. (1) and (2) for $t_r = 5$. This could represent the situation of a disease such as the flu, which has a mean recovery time of five days. Also, in Fig. 5 we compare these results with the $t_r = 1$ case. Note that results for different recovery times t_r do not qualitatively differ. However, for fixed f_1, the epidemic phase becomes wider when t_r increases. This is because the infected individuals have more time to propagate the disease, and thus the contact times must be shorter (or have larger disorder intensities) to move the disease to a non-epidemic phase. The recovery time is an important factor that needs to be accounted for in the implementation of our epidemic-avoiding strategy, and it varies depending on the type of disease.
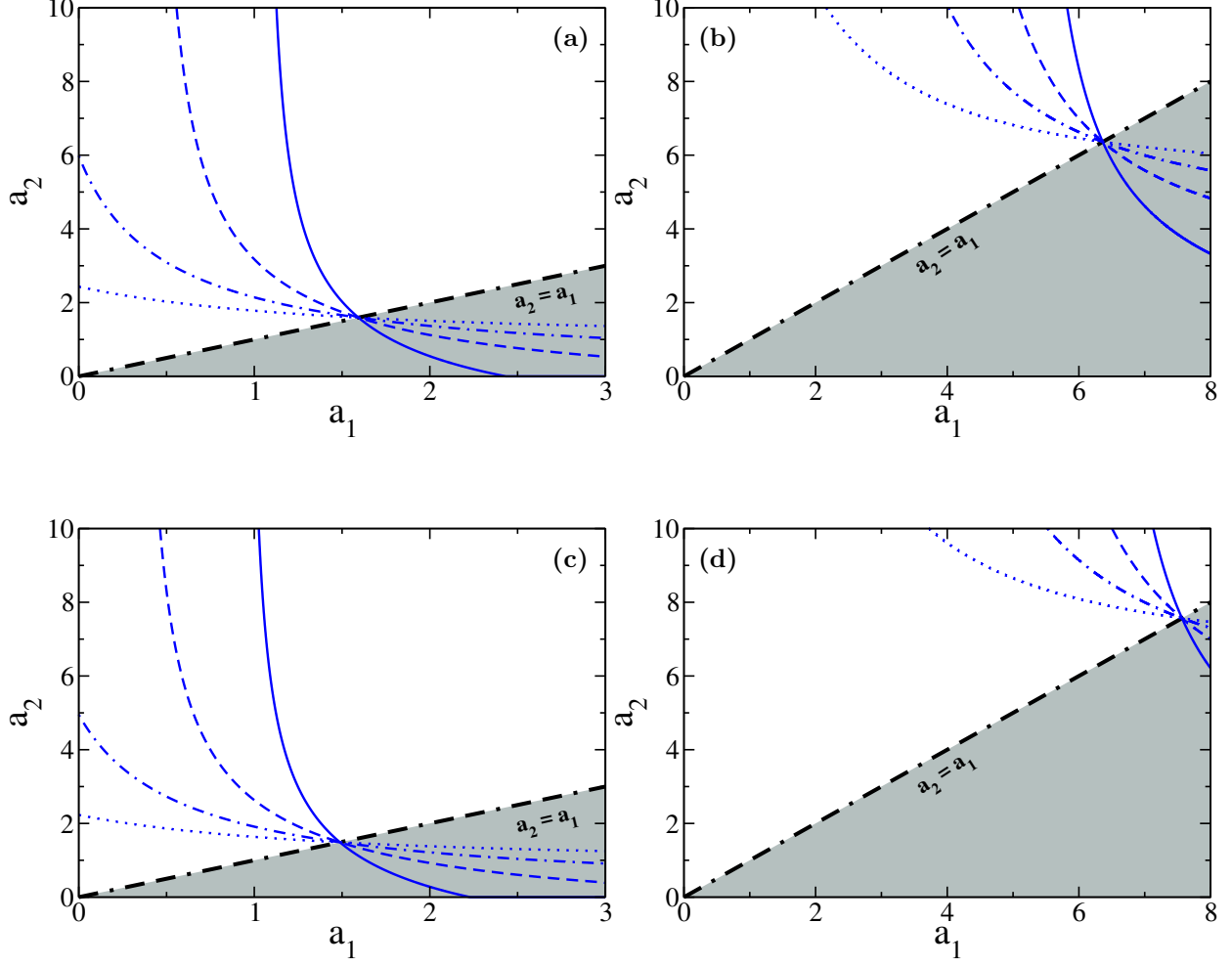
FIG. 5: Phase space of the system projected on the (a_1, a_2) plane, for different densities of close contacts: $f_1 = 0.2$ ($\cdots\cdots$), $f_1 = 0.4$ ($-\cdot-$), $f_1 = 0.6$ ($---$) and $f_1 = 0.8$ (——). The upper figures correspond to $\beta = 0.5$ and an ER network with $k_{\min} = 0$, $k_{\max} = 40$ and $\langle k \rangle = 4$ for (a) $t_r = 1$ and (b) $t_r = 5$. The lower figures correspond to $\beta = 0.25$ and a SF network with $k_{\min} = 2$, $k_{\max} = 250$, $\lambda = 2.5$ and exponential cutoff $k_c = 50$ for (c) $t_r = 1$ and (d) $t_r = 5$. Note that the critical intensities take greater values to counter the increase of the recovery times.

IV. ANALYSIS FOR THE DISTRIBUTION $P'(\omega) = 1/(a_1' \omega^{1.6})$

Some "face-to-face" experiments have studied the contact behavior of individuals at conference-like reunions. The duration of these interactions is accurately reflected by a distribution

$P'(\omega) \propto \omega^{-1.6}$ [31, 33]. For a more realistic analysis, we include this distribution in our model with a density f_1 of close contacts. We make this selection because individuals at conferences usually spend most of their time with the same group of people, a contact pattern that we define to be close. We compare our previous results with those produced by this new distribution, strictly defined by $P'(\omega) = 1/(a_1'\omega^{1.6})$, where $\omega \in [(1+0.6a_1')^{-5/3}, 1]$ and a_1' is the disorder intensity.

As we stated before, now we work with a population in which a density f_1 of the interactions has a contact time distribution $P'(\omega) = 1/(a_1'\omega^{1.6})$ and the density $f_2 = 1 - f_1$ is distributed according to $P(\omega) = 1/(a_2\omega)$. We want to compare this scenario with the previously studied case, which only differs in that the distribution of the density f_1 of contact times is $P(\omega) = 1/(a_1\omega)$. In order to accurately compare these distributions, the normalized contact time ranges must be the same for both and thus, the minimum ω values must be equal. This yields $(1+0.6a_1')^{-5/3} = e^{-a_1}$ and gives a relation between the disorder intensities a_1 and a_1'. For a fixed value of a_1, we compute the corresponding value for a_1' and use these two intensities to obtain the critical values a_{2c} for each case. Then, we plot a_{2c} as a function of a_1 for both cases [see Fig. 6(a)]. This allows a comparison of the results when both distributions have the same range of normalized contact times. We can see that for the distribution $P'(\omega)$, the critical values a_{2c} are smaller than those that were previously obtained for $P(\omega)$, which means that the disease spreads more easily under the distribution $P(\omega)$. We can understand this if we observe Fig. 6 (b), where we show a comparison between the average normalized contact times $f_1\langle\omega\rangle'$ and $f_1\langle\omega\rangle$, corresponding to the density f_1 of contacts distributed according to $P'(\omega)$ and $P(\omega)$, respectively. For any a_1 value $f_1\langle\omega\rangle' < f_1\langle\omega\rangle$, which means that the disease is less likely to propagate through interactions when the contact times are distributed according to $P'(\omega)$, the more realistic distribution of contact times that we defined from the experiments.

V. CONCLUSIONS

In this paper, we study the SIR model for disease spreading over a disordered complex network, in which two types of interactions are defined: close and distant contacts, with larger and shorter mean contact times, respectively. We propose a mitigation strategy consisting in reducing the average contact time of distant interactions (by increasing a_2 in
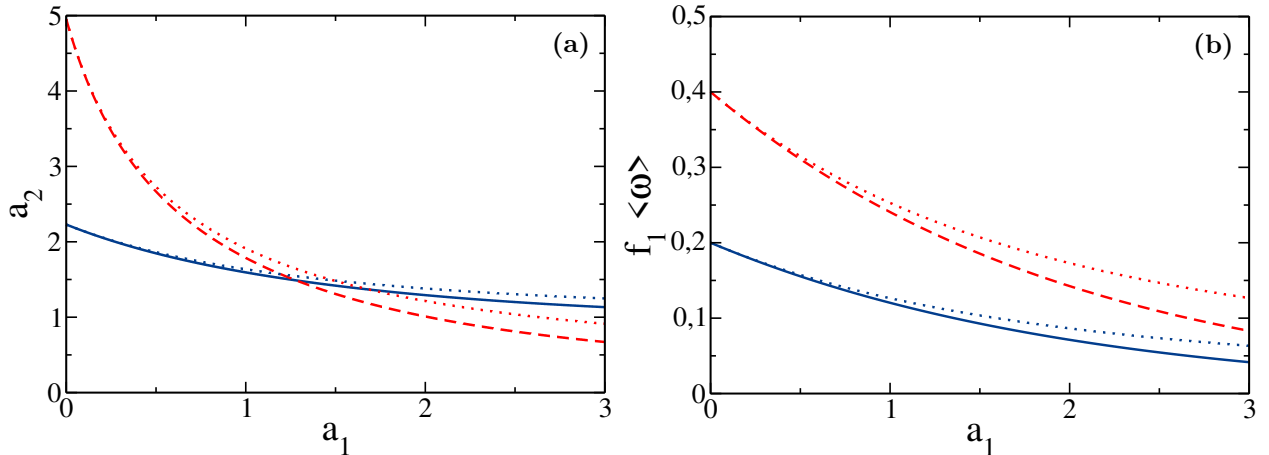
FIG. 6: (a) Critical intensities a_{2c} and (b) average normalized contact times $f_1\langle\omega\rangle$, as functions of a_1, for different densities of close contacts distributed according to $P'(\omega) = 1/(a_1'\omega^{1.6})$: $f_1 = 0.2$ (——) and $f_1 = 0.4$ (- - -). The dotted lines are the corresponding results previously obtained for the distribution of close contacts $P(\omega) = 1/(a_1\omega)$. Disorder intensity a_1 is such that the minimum values of ω coincide for both distributions. Results shown in (a) correspond to a SF network with $k_{\min} = 2$, $k_{\max} = 250$, $\lambda = 2.5$ and exponential cutoff $k_c = 50$, for $\beta = 0.25$ and $t_r = 1$. Note that in (b), for a fixed value of f_1, the difference between average contact times increases with a_1, i.e., when the range of allowed contact times becomes wider.

the model). We find that the strategy is more effective for smaller densities f_1 of close contacts, as the disease is more likely to propagate through them. Also, there is a threshold density $\tilde{f}_1 = T_c/\beta$ of close contacts below which the strategy can prevent the system to enter in an epidemic phase, regardless of the average contact time of close interactions. Using a distribution of close contact times $P'(\omega) = 1/(a_1'\omega^{1.6})$ that adjusts better with some experimental results, we find that the propagation decreases and it is easier to reduce the impact of a disease than when using the theoretical distribution $P(\omega) = 1/(a_1\omega)$.

The analysis carried out here can be extended to interconnected networks, where each network represents a different environment in which interactions take place. As differing networks can have their own degree distribution, this could be an approach for making our close/distant interaction model more realistic and broadly applicable. Since it is well known that such interconnected systems accelerate spreading processes, it is fundamental, in these

cases, to find ways to halt or slow them down.

[1] R. M. Anderson and R. M. May, *Infectious Diseases of Humans: Dynamics and Control* (Oxford University Press, Oxford, 1992).

[2] N. P. A. S. Johnson and J. Mueller, Bull. Hist. Med. **76**, 105 (2002).

[3] C. Fraser, C. A. Donnelly, S. Cauchemez, W. P. Hanage, M. D. Van Kerkhove, T. D. Hollingsworth, J. Griffin, R. F. Baggaley, H. E. Jenkins, E. J. Lyons, *et al.*, Science **324**, 1557 (2009).

[4] S. Merler, M. Ajelli, L. Fumanelli, M. F. C. Gomes, A. Pastore y Piontti, L. Rossi, D. L. Chao, I. M. Longini, M. E. Halloran, and A. Vespignani, Lancet Infect. Dis. **15**, 204 (2015).

[5] M. Fox, "New york is fighting its worst outbreak of measles in decades," (2019).

[6] A. E. van den Bogaard and E. E. Stobberingh, Int. J. Antimicrob. Ag. **14**, 327 (2000).

[7] World Health Organization, "Using climate to predict infectious disease outbreaks: A review," (2004).

[8] A. J. McMichael, R. E. Woodruff, and S. Hales, The Lancet **367**, 859 (2006).

[9] M. Greger, Crit. Rev. Microbiol. **33**, 243 (2007).

[10] M. E. J. Newman, Phys. Rev. E **66**, 016128 (2002).

[11] S. Boccaletti, V. Latora, Y. Moreno, M. Chavez, and D. Hwang, Phys. Rep. **424**, 175 (2006).

[12] M. E. J. Newman, *Networks: An Introduction* (Oxford University Press, 2010).

[13] C. Castellano and R. Pastor-Satorras, Phys. Rev. Lett **105**, 218701 (2010).

[14] R. Pastor-Satorras, C. Castellano, P. Van Mieghem, and A. Vespignani, Rev. Mod. Phys. **87**, 925 (2015).

[15] W. Wang, M. Tang, H. E. Stanley, and L. A. Braunstein, Reports on Progress in Physics **80**, 036603 (2017).

[16] P. Grassberger, Math. Biosci. **63**, 157 (1983).

[17] N. T. J. Bailey, *The Mathematical Theory of Infectious Diseases* (Griffin, London, 1975).

[18] J. C. Miller, Phys. Rev. E **76**, 010101 (2007).

[19] E. Kenah and J. M. Robins, Phys. Rev. E **76**, 036113 (2007).

[20] C. Lagorio, M. V. Migueles, L. A. Braunstein, E. López, and P. Macri, Physica A **388**, 755 (2009).

[21] L. A. Meyers, Bull. Amer. Math. Soc. **44**, 63 (2007).

[22] M. J. Ferrari, S. Bansal, L. A. Meyers, and O. N. Bjørnstad, Proc. R. Soc. London, Ser. B **273**, 2743 (2006).

[23] S. Bansal, B. Pourbohloul, and L. A. Meyers, PLoS Med. **3**, e387 (2006).

[24] M. A. Di Muro, L. G. Alvarez-Zuzek, S. Havlin, and L. A. Braunstein, New J. Phys. **20**, 083025 (2018).

[25] T. Gross, C. J. Dommar D'Lima, and B. Blasius, Phys. Rev. Lett. **96**, 208701 (2006).

[26] C. Lagorio, M. Dickison, F. Vazquez, L. A. Braunstein, P. A. Macri, M. V. Migueles, S. Havlin, and H. E. Stanley, Phys. Rev. E **83**, 026102 (2011).

[27] C. Buono, C. Lagorio, P. A. Macri, and L. A. Braunstein, Physica A **391**, 4181 (2012).

[28] L. D. Valdez, P. A. Macri, and L. A. Braunstein, Phys. Rev. E **85**, 036108 (2012).

[29] C. Buono, F. Vazquez, P. A. Macri, and L. A. Braunstein, Phys. Rev. E **88**, 022813 (2013).

[30] K. Eastwood, D. N. Durrheim, M. Butler, and E. A. Jon, Emerg. Infect. Dis. **16**, 1211 (2010).

[31] C. Cattuto, W. V. den Broeck, A. Barrat, V. Colizza, J. F. Pinton, and A. Vespignani, PLoS ONE **5**, e11596 (2010).

[32] M. Karsai, M. Kivelä, R. K. Pan, K. Kaski, J. Kertész, A. L. Barabási, and J. Saramäki, Phys. Rev. E **83**, 025102 (2011).

[33] J. Stehleé, A. Barrat, C. Cattuto, J. F. Pinton, L. Isella, and W. V. den Broeck, J. Theor. Biol. **271**, 166 (2011).

[34] L. D. Valdez, C. Buono, P. A. Macri, and L. A. Braunstein, FRACTALS **21**, 1350019 (2013).

[35] M. Molloy and B. Reed, Random Struct. Algor. **6**, 161 (1995).

[36] L. A. Braunstein, Z. Wu, Y. Chen, S. V. Buldyrev, T. Kalisy, S. Sreenivasan, R. Cohen, E. Lpez, S. Havlin, and H. E. Stanley, International Journal of Bifurcation and Chaos **17**,

2215 (2007).

[37] M. E. J. Newman, S. H. Strogatz, and D. J. Watts, Phys. Rev. E **64**, 026118 (2001).

[38] M. E. J. Newman, SIAM Rev. **45**, 167 (2003).